AD-A033 859 NAVAL RESEARCH LAB WASHINGTON D C F/G 20/3
MAGNETIC COMPRESSION OF CHARGE-NEUTRALIZED ION BEAMS.(U)
NOV 76 D MOSHER
UNCLASSIFIED NRL-MR-3413 NL

1 OF 1
AD A033859

END
DATE FILMED
2-77

NRL Memorandum Report 3413

Magnetic Compression of Charge-Neutralized Ion Beams

DAVID MOSHER

Plasma Technology Branch
Plasma Physics Division

November 1976

This research was sponsored by the Defense Nuclear Agency under subtask T99QAXLA014, work unit 05, work unit title Advanced Concepts.

NAVAL RESEARCH LABORATORY
Washington, D.C.

SECURITY CLASSIFICATION OF THIS PAGE (When Data Entered)

REPORT DOCUMENTATION PAGE

READ INSTRUCTIONS BEFORE COMPLETING FORM

1. REPORT NUMBER: NRL Memorandum Report 3413
2. GOVT ACCESSION NO.
3. RECIPIENT'S CATALOG NUMBER

4. TITLE (and Subtitle): MAGNETIC COMPRESSION OF CHARGE-NEUTRALIZED ION BEAMS
5. TYPE OF REPORT & PERIOD COVERED: Final report, on one phase; work continues.
6. PERFORMING ORG. REPORT NUMBER

7. AUTHOR(s): David Mosher
8. CONTRACT OR GRANT NUMBER(s)

9. PERFORMING ORGANIZATION NAME AND ADDRESS: Naval Research Laboratory, Washington, D.C. 20375
10. PROGRAM ELEMENT, PROJECT, TASK AREA & WORK UNIT NUMBERS

11. CONTROLLING OFFICE NAME AND ADDRESS: Defense Nuclear Agency, Washington, D.C. 20305
12. REPORT DATE: November 1976
13. NUMBER OF PAGES: 35

14. MONITORING AGENCY NAME & ADDRESS (if different from Controlling Office): NRL-MR-3413
15. SECURITY CLASS. (of this report): UNCLASSIFIED
15a. DECLASSIFICATION/DOWNGRADING SCHEDULE

16. DISTRIBUTION STATEMENT (of this Report)

Approved for public release; distribution unlimited.

17. DISTRIBUTION STATEMENT (of the abstract entered in Block 20, if different from Report)

18. SUPPLEMENTARY NOTES

This research was sponsored by the Defense Nuclear Agency under subtask T99QAXLA014, work unit 05, work unit title Advanced Concepts.

19. KEY WORDS (Continue on reverse side if necessary and identify by block number)

Ion beams
Reflex triodes
Magnetic compression

20. ABSTRACT (Continue on reverse side if necessary and identify by block number)

Magnetic compression of a cold, charge-neutralized ion beam due to passage through a slowly-varying magnetic-mirror field is studied. Conditions on the field and beam parameters are derived which permit the beam to be compressed to order-of-magnitude higher current densities while preserving the laminar nature of the flow. Effects associated with rotation, beam convergence, and velocity shear in the incident beam, and those due to self fields are included in the analysis. Utilization of compressed beams extracted from reflex triodes and ion diodes for heating of thermonuclear plasmas is discussed.

DD FORM 1 JAN 73 1473 EDITION OF 1 NOV 65 IS OBSOLETE S/N 0102-014-6601

SECURITY CLASSIFICATION OF THIS PAGE (When Data Entered)

CONTENTS

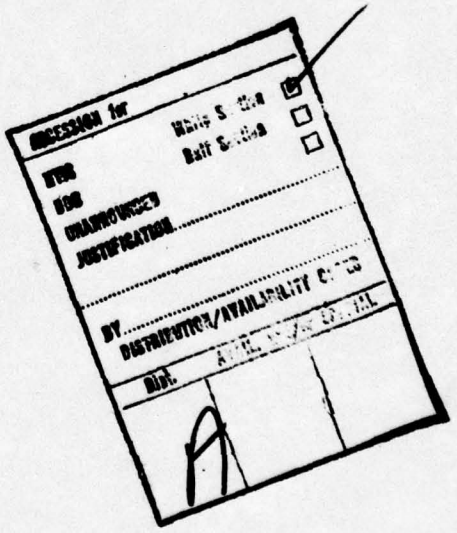

MAGNETIC COMPRESSION OF CHARGE-NEUTRALIZED ION BEAMS

I. INTRODUCTION

High-power relativistic-electron-beam generators have recently been used to create intense ion beams characterized by 20-50 ns, 20-200 kA pulses of .5-1.5 MeV protons or deuterons with 100-1000 cm^2 cross-sectional areas.[1-5] Such beams may be of value to controlled fusion research[1] in the areas of plasma heating,[6] magnetic confinement (by the creation of field-reversing ion layers[7]), and pellet fusion.[8] Usefulness in these areas would benefit from compression of the ion beams to current densities higher than the .1-1 kA/cm^2 indicated by the above parameters. Two accelerator configurations, the magnetically-insulated[3] and self-pinched[4] diodes, permit one to achieve higher current densities by geometric focusing.[9] This technique cannot easily be applied in a reflex-triode geometry[3] in which a charge-neutralized ion beam is extracted into a drift region along a constant axial magnetic field. In the work to be presented here, the conditions under which such a beam can be radially compressed by a gradual increase in the applied magnetic field is investigated. A long magnetic-field compression length is desired in order that the ions remain closely tied to the field lines, i.e. the laminar, paraxial nature of the beam flow is to be preserved as much as practical during compression. In this way, the bulk of the beam kinetic energy remains associated with motion parallel to the applied

Note: Manuscript submitted November 8, 1976.

field, the ion gyroradius stays small in comparison to the beam radius, and maximum amplification in current density is achieved. In a sense, the goals are the opposite of those associated with the creation of a rotating ion ring by passing a cold, paraxial beam extracted from a reflex triode through a sharp magnetic cusp.[7]

Cold ion and electron fluid equations are solved for passage through a specific magnetic-mirror configuration. The compressed-beam radius and the energy associated with motion transverse to the field in a high axial-field region beyond the mirror area are calculated as a function of the mirror ratio, mirror length, applied field strength and ion-beam parameters. Conditions which insure the desired smallness of these two quantities are determined. The effects of initial beam rotation, convergence, and velocity shear as well as self-field effects are considered in the analysis. Finally, an example of how magnetic compression of ion beams may be used to heat a thermonuclear plasma is presented.

II. SOLUTION OF THE FLUID EQUATIONS OF MOTION

The fluid flow of a cold, charge-neutralized ion beam (charge state Z) in an external magnetic mirror field is now considered. Cylindrically-symmetric, steady-state equations in the small electron-gyroradius limit are studied. A self-consistent electric field determined from the quasi-neutral assumption ($n_e = Zn_i = Zn$) is included. Electron temperature and inertia are ignored. However, electron-temperature effects are considered in the appendix where their neglect in the present analysis is discussed. Consideration is limited to magnetic fields which change sufficiently slowly to maintain most of the ion kinetic energy in motion along the field lines. This limitation allows one to neglect the finite-gyroradius contribution of the ion-stress tensor[10] and provides simplifying assumptions for solution of the equations of motion. Field and ion-beam conditions which insure the validity of these approximations are derived a posteriori. For the present, the self-magnetic fields associated with the beam are also ignored so that

$$\vec{\nabla} \times \vec{B} = \vec{\nabla} \cdot \vec{B} = 0$$

determines the applied magneto-static field. The ion density, electric field, ion and electron fluid velocities ($\vec{V}$ and $\vec{v}$) are then determined from

$$\vec{\nabla} \cdot (n\vec{V}) = \vec{\nabla} \cdot (Zn\vec{v}) = 0 \qquad (1)$$

$$m_i \vec{V} \cdot \vec{\nabla} \vec{V} = Ze\ (\vec{E} + \vec{V} \times \vec{B}) \qquad (2)$$

$$0 = Ze\,(\vec{E} + \vec{v} \times \vec{B}) \tag{3}$$

$$\vec{\nabla} \times \vec{E} = 0 \quad ; \quad \vec{E} = -\vec{\nabla}\varphi. \tag{4}$$

Since Eq. (4) requires $E_\theta = 0$, the θ-component of Eq. (3),

$$v_r B_z = v_z B_r \tag{5}$$

states that the electron fluid follows the line of force. Taking the scaler product of Eq. (3) with $\vec{B}$ results in

$$B_r \frac{\partial \varphi}{\partial r} + B_z \frac{\partial \varphi}{\partial z} = 0 \tag{6}$$

so that φ is constant along a line of force. Magnetic fields of interest take the form

$$\vec{B} = \vec{\nabla} \times (\hat{e}_\theta A_\theta)$$

so that

$$\varphi = f(rA_\theta) \tag{7}$$

satisfies Eq. (6). The r-component of Eq. (3) yields

$$v_\theta = -E_r/B_z. \tag{8}$$

Manipulation of the electron continuity equation, Eq. (5), and $\vec{\nabla} \times \vec{B} = 0$ leads to

$$\left(B_r \frac{\partial}{\partial r} + B_z \frac{\partial}{\partial z}\right) \frac{nv_z}{B_z} = 0$$

so that

$$\frac{nv_z}{B_z} = g(rA_\theta). \tag{9}$$

Solutions of the ion equations are more complicated. Some aspects of analysis are simplified by noting that any two components of Eq. (2) can be replaced by statements of conservation of canonical angular momentum and energy of a fluid element.

$$\left(V_r \frac{\partial}{\partial r} + V_z \frac{\partial}{\partial z}\right)\left[r\left(V_\theta + \frac{Ze}{m_i} A_\theta\right)\right] = 0 \tag{10}$$

$$\left(V_r \frac{\partial}{\partial r} + V_z \frac{\partial}{\partial z}\right)\left(\tfrac{1}{2} m_i V^2 + Ze\varphi\right) = 0 \tag{11}$$

Specific forms for A_θ and φ which satisfy the requirements of the present problem are chosen. For simplicity, B_z depending only on z is chosen so that

$$A_\theta = \tfrac{1}{2}\, rB_z(z) \tag{12}$$

and

$$B_r = -\tfrac{1}{2}\, rB_z' \tag{13}$$

where the prime denotes differentiation with respect to z. The simplest form for φ is then

$$\varphi(r,z) = SrA_\theta = \tfrac{1}{2} Sr^2 B_z \tag{14}$$

where S is a constant.

The beam is injected at $z = 0$ into a constant solenoidal field $\vec{B} = B_o \hat{e}_z$. Solutions are sought in the field-compression region $0 \le z \le L$ and in the high-field solenoidal region $z > L$ in which $\vec{B} = B_f \hat{e}_z = AB_o \hat{e}_z$.

The plane $z = 0$ may be identified with that of the transmission cathode of a reflex triode. A radial electric field in the $z = 0$ plane (permitted by Eq. (14)) may exist when the cathode is virtual because of low-energy-electron space-charge accumulation but is likely to be negligible when a thin-foil transmission cathode is employed. In the latter case, $\varphi = 0$ solutions to the equations of motion are appropriate since any conducting cathode plasma would limit the radial electric field to very small values.

Assuming a rigid-rotor behavior for the ion flow

$$V_\theta = \omega(z) r \tag{15}$$

leads to a solution of Eq. (10) of the form

$$V_r = - \frac{r}{2} \frac{w'}{w} V_z \tag{16}$$

where

$$w(z) = \omega + \tfrac{1}{2} \Omega$$

and

$$\Omega(z) = \frac{Ze}{m_i} B_z(z).$$

If $\rho(z)$ represents the radius of a fluid element as it flows along z, then integration of Eq. (16) using

$$\frac{d\rho}{dz} = \frac{V_r}{V_z}$$

results in

$$\rho^2 w = \text{constant} \quad . \tag{17}$$

Substitution from Eqs. (13) and (14) into the z-component of Eq. (2) leads to

$$\left(\frac{V_r}{V_z}\frac{\partial}{\partial r} + \frac{\partial}{\partial z}\right) V_z^2 = \Omega' r^2 \ (\omega - s) \quad . \tag{18}$$

Employing Eq. (16) and integrating, one obtains

$$V_z^2 = V_o^2 \left[1 - \nu(z) r^2\right] \tag{19}$$

where

$$\frac{d}{dz}\left(\frac{\nu}{w}\right) = - \frac{\Omega'(\omega - s)}{V_o^2 w} \tag{20}$$

and the constant V_o is the ion-flow velocity at $r = 0$. The initial value $\nu(0)$ can be determined from the radial electric field at $z = 0$ when the ion motion between anode and transmission cathode is purely axial. In that case, conservation of energy requires

$$\tfrac{1}{2} m_i V_z^2(r,o) + Ze\varphi(r,o) = Ze\varphi_a \tag{21}$$

where φ_a is the anode potential. Substituting from Eqs. (14) and (19) evaluated at $z = 0$ and collecting terms in powers of r results in

$$V_o^2 = 2Ze\varphi_a / m_i \quad ; \quad \nu(0) = \Omega_o S / V_o^2 \tag{22}$$

where $\Omega_c = \Omega(0)$. Equation (22) may be applicable when the triode-current self magnetic field is small compared to the applied axial

field. When motion transverse to the applied field is not ignorable, determination of $\vec{V}$ at $z = 0$ requires a complicated analysis of ion and electron motion coupled with a 2-dimensional solution of Poisson's equation.

The ion continuity equation may be solved by substitution for V_r from Eq. (16). The resulting equation

$$\frac{w}{w'}\frac{\partial}{\partial z}(r^2 n V_z) = \frac{r}{2}\frac{\partial}{\partial r}(r^2 n V_z)$$

has as a solution

$$n(r,z)V_z = \frac{1}{r^2} f(r^2 w) \tag{23}$$

with f determined from the radial distribution of the incident beam

$$f(r^2 w_o) = r^2 n(r,0) V_z(r,0).$$

For $n(r,0) = n_o$ = constant when $r \leq R_o$ and equal to zero otherwise, and $V_z(r,0) = V_o$,

$$n(r,z) = \frac{n_o R_o^2}{R^2(z)} \frac{1}{1-\nu(z)r^2} \tag{24}$$

for $r \leq R(z)$, while $n(r,z) = 0$ for $r > R(z)$. Equation (17) is the form

$$R^2(z)w(z) = R_o^2 w_o \tag{25}$$

has been used to eliminate w(z) from Eq. (23). The quantity R(z) is the radius of the beam edge with $R_o = R(0)$, $w_o = \omega_o + \frac{1}{2}\Omega_o$, and $\omega_o = \omega(0)$.

Determination of $\omega(z)$ or w(z) is all that is required to complete the solution of the ion equations of motion. Manipulation of the

r-component of Eq. (2) and substituting from Eq. (18) leads to

$$V_z^2 \left(\frac{V_r}{V_z} \frac{\partial}{\partial r} + \frac{\partial}{\partial z} \right) \left(\frac{V_r}{V_z} \right) = r(\omega^2 + \Omega\omega - s\Omega) \qquad (26)$$
$$-\tfrac{1}{2}\Omega'(\omega - s) r^2 \left(\frac{V_r}{V_z} \right)$$

which, upon evaluation of $\frac{V_r}{V_z}$ from Eq. (16) and V_z from Eq. (19) admits of solutions of the form $\omega = \omega(z)$ only when the cubic terms in r can be neglected. The two terms in question can be ignored when

$$| \nu r^2 | \ll 1 \quad ; \quad \Omega' r \left| \frac{V_r}{V_z} \right| \ll \Omega \qquad (27)$$

for all $z \geq 0$ and $r \leq R(z)$. It will be shown later that the conditions of Eq. (27) are satisfied for sufficiently-slowly-varying magnetic fields provided they are satisfied at $z = 0$. The condition $| \nu(0) R_o^2 | \ll 1$ is satisfied by the realistic limitation of having small radial electric fields at $z = 0$ compared to the axial accelerating field in the triode and by requiring that ion motion in the triode not be dominated by self-fields. The condition $| V_r/V_z |_{z=0} \ll 1$ states that the incident beam is only weakly convergent or divergent and is satisfied by the same field restrictions as the $\nu(0)R_o^2$ condition.

Elimination of the r^3 terms in Eq. (26) leads to

$$\frac{1}{w} \frac{d^2 w}{dz^2} - \frac{3}{2} \left(\frac{1}{w} \frac{dw}{dz} \right)^2 = - \frac{2}{V_o^2} \left[w^2 - \Omega \left(\frac{\Omega}{4} + s \right) \right] . \qquad (28)$$

The initial value of $\frac{dw}{dz}$ is determined by the radial convergence or divergence of the beam according to

$$\frac{w'(0)}{w(0)} = -\frac{2}{r}\frac{V_r(r,0)}{V_o} \tag{29}$$

since $V_z(r,0) \simeq V_o$ is correct to lowest order in νr^2. Since V_r/V_z is nearly proportional to r, the incident beam either converges to or diverges from a point focus on the axis of symmetry. Denoting the axial location of this point by z_f, $w'(0)$ is given by

$$w'(0) = 2w(0)/z_f \quad . \tag{30}$$

Equations (20) and (28) may be solved numerically for a given set of initial conditions and a specified $B_z(z)$. Figure 1 illustrates the evolution of the beam-envelope radius R(z) (obtained from w(z) using Eq. (25)), $\omega(z)$, and $\nu(z)$ for the case of parallel ($\omega_o = 0$; $z_f = \infty$), shear-free ($\nu(0) = 0$) injection of ions in the absence of electric fields. The magnetic field variation, also shown in the figure, is of the form

$$B_z = \frac{B_o}{2}\left[A+1 - (A-1)\cos(\pi z/L)\right] \tag{31}$$

for $0 \le z \le L$, while $B_z = AB_o$ for $z > L$. A mirror-ratio of 6 and a mirror length $L\Omega_o/V_o = 10$ were chosen for the illustrated calculation.

Although ions are injected parallel to the field lines, inertia causes them to deviate from the lines of force as the field is compressed. When the distance L over which the field varies is short, a large fraction of the ion kinetic energy is transferred to motion transverse to the lines of force after passage through the mirror. Large radial excursions associated with the transverse energy reduce the effective beam compression since R_M, the maximum of R(z) in the regime

$z > L$, can be comparable to R_o. When L is sufficiently large, ions can closely follow the gently-curving field lines and the transverse energy fraction stays small. In this case, R_M/R_o approaches $A^{-\frac{1}{2}}$, the field-line radial-compression ratio. The particular case shown in Fig. 1 shows a 5-fold increase in current density $\sim(R_o/R_M)^2$ for a 6-fold increase in magnetic-field strength. The dependence of R_M and the transverse-energy component on field and beam parameters is discussed in the next section.

III. DEPENDENCE OF TRANSVERSE ENERGY AND RADIAL COMPRESSION ON FIELD AND BEAM PARAMETERS

The total power convected by the beam in the form of ion kinetic energy across any z = constant plane is

$$P = \int_0^{R(z)} \tfrac{1}{2} m_i V^2 \cdot n V_z \cdot 2\pi r dr$$

$$= \tfrac{1}{2} m_i V_o^2 \int_0^R n V_z \left[1 - \nu r^2 + \frac{\omega^2 r^2}{V_o^2} + \tfrac{1}{4} \left(\frac{w'}{w} \right)^2 r^2 \right] \cdot 2\pi r dr$$

$$= \tfrac{1}{2} m_i V_o^2 \left\{ \Phi + \frac{1}{w} \left[\frac{\omega^2}{V_o^2} + \tfrac{1}{4} \left(\frac{w'}{w} \right)^2 - \nu \right] I \right\} \qquad (32)$$

where V_r^2 was evaluated to lowest order in νr^2 by replacing V_z with V_o and

$$\Phi = \int_0^R n V_z \cdot 2\pi r dr \quad ; \quad I = w \int_0^R n V_z \cdot 2\pi r^3 dr \qquad (33)$$

Substituting from Eq. (23) into Eq. (33), setting $u = r^2 w$ and using Eq. (25) to convert the upper limit of integration results in

$$\Phi = \pi \int_0^{R_o^2 w_o} f(u) \frac{du}{u} \quad ; \quad I = \pi \int_0^{R_o^2 w_o} f(u)\, du$$

where f(u) is defined in Eq. (23). Therefore, both Φ and I are constants which depend only on the radial distribution of the beam at z = 0. For the uniform-current-density case described by Eq. (24), f(u) is proportional to u and

$$I = \tfrac{1}{2} R_o^2 w_o \Phi. \qquad (34)$$

The quantity multiplying I in Eq. (32) can also be shown to be constant when electric-potential changes are negligible compared to the

ion kinetic energy. In that case, Eq. (11) states that V^2 is constant following the ion fluid. Specifically, at the edge of the beam $r = R(z)$:

$$V^2(R,z) = V_o^2 \left[1 - \nu R^2 + \omega^2 R^2 + \frac{R^2}{4} \left(\frac{w'}{w} \right)^2 \right] \tag{35}$$

will be a constant to order νR^2. Use of Eq. (25) then results in

$$\frac{1}{w} \left[\frac{\omega^2}{V_o^2} + \frac{1}{4} \left(\frac{w'}{w} \right) - \nu \right] = \text{constant.} \tag{36}$$

The power P is then also a constant. For uniform incident current density, it is given by

$$P = P_o \left\{ 1 + \tfrac{1}{2} R^2 \left[\frac{\omega^2}{V_o^2} + \frac{1}{4} \left(\frac{w'}{w} \right)^2 - \nu \right] \right\} \tag{37}$$

where $P_o = \frac{1}{2} m_i V_o^2 \Phi$. The power can be divided into those associated with motions in the z-direction and perpendicular-to-z direction according to

$$P_{||}(z) = P_o \left(1 - \tfrac{1}{2} R^2 \nu\right) \tag{38}$$

$$P_\perp(z) = \tfrac{1}{2} P_o R^2 \left[\frac{\omega^2}{V_o^2} + \frac{1}{4} \left(\frac{w'}{w} \right)^2 \right]$$

$$= P - P_{||}(z) \, . \tag{39}$$

Since P is constant, $\Delta P_\perp = -\Delta P_{||}$ or

$$P_\perp(z) = P_{\perp o} + \tfrac{1}{2} P_o \left[R^2(z)\nu(z) - R_o^2 \nu(0) \right] \tag{40}$$

where

$$P_{\perp o} = \tfrac{1}{2} P_o R_o^2 \left(\frac{\omega_o^2}{V_o^2} + \frac{1}{z_f^2} \right). \tag{41}$$

Thus, a knowledge of the change in νR^2 is sufficient to characterize the partition of beam energy between motion along and transverse to the axis of symmetry of the beam. In the region $z > L$, the quantities $P_{||}$ and $P_{\perp}$ are also constant since νR^2 is by virtue of Eqs. (18) and (25). This final value of $P_{\perp}$ is

$$P_{\perp f} = P_{\perp o} + \tfrac{1}{2} P_o \left[(\nu R^2)_f - \nu(0) R_o^2 \right] . \tag{42}$$

The radial excursion in the $z > L$ regime can be determined in terms of $P_{\perp f}$. From Eqs. (25) and (39)

$$\frac{1}{w} \left[\frac{\omega^2}{V_o^2} + \tfrac{1}{4} \left(\frac{w'}{w} \right)^2 \right] = \frac{2P_{\perp f}}{P_o w_o R_o^2} . \tag{43}$$

Extremum values of $R(z)$ are obtained by solving the quadratic equation in w which results from setting $w' \sim V_r = 0$ and replacing ω with $w - \frac{1}{2}\Omega_f = \omega - \frac{1}{2} A\Omega_o$. Use of Eq. (25) then gives

$$\left(\frac{R_{M,m}}{R_o} \right)^2 = \frac{1}{A} \frac{1+2\omega_o/\Omega_o}{1+\epsilon \mp (2\epsilon+\epsilon^2)^{\frac{1}{2}}} . \tag{44}$$

In Eq. (44), R_M is obtained using the minus sign while R_m, the minimum beam radius in the $z > L$ regime, is determined with the plus sign. The quantity of ϵ is given by

$$\epsilon = \frac{2P_{\perp f} V_o^2}{P_o w_o R_o^2 \Omega_f} = \frac{4P_{\perp f}}{AP_o} \left(\frac{V_o}{R_o \Omega_o} \right)^2 \frac{1}{1+2\omega_o/\Omega_o} . \tag{45}$$

Therefore, the two primary quantities of interest $P_{\perp f}$ and R_M/R_o may be determined from initial conditions and $(\nu R^2)_f$ which, in turn, is calculated by simultaneous numerical integration of Eqs. (20) and (28).

Figure 2 shows the limits to radial excursion and values of $(\nu R^2)_f$ for $z > L$ as a function of mirror length for various mirror ratios. Initial conditions are as described for Fig. 1, i.e. $\nu(0) = \omega_o = V_r(r,0) = S = 0$. As an example of the results shown in this figure, consider a 10 cm-radius beam of 1 MeV ions accelerated in a reflex-triode with $B_o = 5$ kG. This beam can be compressed a factor-of-9 in area with less than a 1% transfer of energy into transverse motion provided that the $A = 10$ magnetic compression occurs over a length $L \geq 4$m.

We next consider how injection of a beam with non-zero transverse kinetic energy alters the compression results already presented. Figure 3 shows the variation in R_M and $(\nu R^2)_f$ with initial frequency of rotation ω_o for $L\Omega_o/V_o = 20$ and various field-compression ratios while maintaining $V_r(r,0) = \nu(0) = S = 0$. The quantity $P_{\perp f}$ may be determined from the figure and Eq. (33) in the form

$$\frac{P_{\perp f}}{P_{\perp o}} = 1 + \frac{(\nu R^2)_f (V_o/R_o\Omega_o)^2}{\omega_o^2/\Omega_o^2} \quad .$$

For positive initial rotation with respect to Ω_o, the final value of $P_\perp$ is seen to be approximately A+1 times the initial value while R_M/R_o is correspondingly larger than the value obtained in the absence of initial rotation. Increases in $P_\perp$ due to initial negative rotation are less and values of R_M/R_o slightly below the field-compression value are calculated. It is also predicted that ω_o/Ω_o values near - .05 result in final values of $P_\perp$ less than that occurring in the absence of initial rotation. Figure 3 therefore indicates that a small, negative, initial rotation of the beam (induced by configuring the triode in a way

that causes a positive radial electric field to exist between anode and transmission cathode) may allow higher compression than parallel beam injection without increasing the final value of $P_\perp$.

Figure 4 shows the variation in R_M and $(\nu R^2)_f$ due to an initial radial-velocity component for $\omega_o = S = 0$. The initial value $\nu(0)$ was determined by assuming that $V_r(r,0)$ is produced only by the self-magnetic field associated with the triode current. If the radial electric field in the accelerating region is ignored so that the plane $z = 0$ is an equipotential, then all ions cross this plane with the same energy. Therefore

$$V_r^2(r,0) + V_z^2(r,0) = \text{constant}.$$

Substituting from Eqs. (19), (29), and (30) results in $\nu(0) = z_f^{-2}$ to lowest order in $\nu(0)r^2$. The final value of $P_\perp$ for this case is then

$$\frac{P_{\perp f}}{P_{\perp o}} = (\nu R^2)_f \frac{z_f^2}{R_o^2} \quad ; \quad z_f^{-1} \neq 0$$

from Eqs. (40) and (41). Examination of Fig. 4 shows that for initially-divergent beams (positive abscissa in the figure), the final value of $P_\perp$ is approximately $AP_{\perp o}$ and is somewhat less for initially convergent beams. Interestingly, an initial radial velocity has little effect on the final radial compression of the beam for all but small values of A. Some small degree of beam focussing may be preferred to parallel injection in order to minimize $P_{\perp f}$ for high values of field compression.

IV. SELF-MAGNETIC-FIELD AND EQUATION-OF-MOTION SMALLNESS REQUIREMENTS

Conditions are determined which insure that the self-magnetic field in the drifting beam and the neglected terms in the equation of motion do not strongly effect the calculated compression. The self field is determined by calculating the total current density using results of Section II. Denoting the self-field by $\vec{b}$

$$\vec{\nabla} \times \vec{b} = 4\pi Zen(\vec{V}-\vec{v}) \tag{46}$$

or, in component form using Eqs. (5), (8), and (16),

$$\frac{\partial b_\theta}{\partial z} + 2\pi Zen \cdot r \left(\frac{w'}{w} V_z - \frac{\Omega'}{\Omega} v_z \right) \tag{47}$$

$$\frac{\partial b_r}{\partial z} - \frac{\partial b_z}{\partial r} = 4\pi Zen \cdot r \ (\omega + S) \tag{48}$$

$$\frac{1}{r} \frac{\partial}{\partial r} r b_\theta = 4\pi Zen(V_z - v_z). \tag{49}$$

For the density distribution of Eq. (24) and the condition $v_z(0) = V_z(0) = V_o$

$$nV_z = n_o V_o \frac{w}{w_o} \quad ; \quad nv_z = N_o V_o \frac{\Omega}{\Omega_o} .$$

Substituting into Eq. (47) or Eq. (49) and integrating leads to

$$b_\theta = 2\pi J_o r \left(\frac{w}{w_o} - \frac{\Omega}{\Omega_o} \right) \tag{50}$$

where $J_o = Zen_o V_o$. The long axial scale lengths compared to those for radial variations allows one to approximate b_z by neglecting the

$\frac{\partial b_r}{\partial z}$ term in Eq. (48) with the result that

$$b_z \simeq -2\pi Zen(\omega+S)r^2 \quad . \tag{51}$$

Then, from $\vec{v}\cdot\vec{b} = 0$,

$$b_r \simeq \frac{\pi}{2} Ze[n(\omega+S)]'r^3 \quad . \tag{52}$$

It is required that the self-fields do not strongly perturb the calculated ion-fluid flow. Statements of this condition from Eq. (2) are

$$| V_\theta B_z | \gg | V_z b_\theta | \qquad \text{and} \qquad | V_\theta B_r | \gg | V_r b_\theta |$$

for all values of z and $r \leq R(z)$. Numerical evaluation of velocity and field quantities for a wide variety of initial conditions, beam, and field parameters demonstrates that the condition

$$B_o \Omega_o \gg 2\pi J_o V_o \tag{53}$$

is sufficient to satisfy these two inequalities. In the same way, numerical evaluation of the quantities in Eq. (27) results in the sufficiency condition

$$3R_o^2 A^2 V_o \ll L^3 \Omega_o \quad . \tag{54}$$

Equation (54) is an empirical relation derived through evaluation of Eq. (27) for various values of L and A. Since this relation insures $| \nu R^2 | \ll 1$, its satisfaction also implies small final values of $P_\perp$ and values of R_M/R_o close to $A^{-\frac{1}{2}}$ provided that $P_{\perp o}$ is small.

V. DISCUSSION OF RESULTS

It has been demonstrated theoretically that a neutralized ion beam extracted from a reflex triode can be magnetically focussed to an order-of-magnitude higher current density by passage through a magnetic mirror. If the incident beam has only a small fraction of its kinetic energy in motion transverse to the magnetic field, the compressed beam will also have a small fraction in transverse motion provided that the scale-length L over which the field varies is sufficiently large. A general condition which L must satisfy is given by Eq. (54). Final transverse-energy components for various initial conditions and values of L and A are illustrated in Figs. 2-4. Small final values of $P_\perp$ also insure small radial excursions of the compressed beam about the radius, $R_o/A^{\frac{1}{2}}$ with specific dependences determined by Eq. (44).

A second general condition which the field and beam parameters must satisfy is given by Eq. (53). Satisfying this inequality insures that the self-magnetic field of the beam will be insufficient to strongly alter the predicted compression values. Existing reflex-triode experiments[2,3] already utilize applied magnetic fields which satisfy a similar condition in order to insure that the extracted beam have most of its kinetic energy in axial motion.

An example of how the technique presented in this work might be applied to a proposed fusion-reactor concept is now presented. Dawson, et. al.[11] have suggested that a solenoidal magnetic field of about 500 kG confining a kilometer-long, 1 cm-radius plasma may be viable as a fusion reactor. Ott and Sudan [6] argue that an ion beam propagated

along the plasma column could heat the plasma to thermonuclear temperatures. They determine that a 20 kA/cm^2, 10 MeV proton beam would be required. Based on present experiments[3], 2 kA/cm^2 could easily be extracted from a reflex triode operating at 10 MV. The current density required to heat the plasma and confining field strength may then be achieved using magnetic compression with B_o = 50 kG, R_o = 3.16 cm, $V_o = 4.36 \times 10^9$ cm/s (for 10 MeV protons), and A = 10. These parameters marginally satisfy Eq. (53) since

$$\frac{B_o \Omega_o}{2\pi J_o V_o} = 4.6.$$

Equation (54) is easily satisfied for L = 3 m and gives $L\Omega_o/V_o \simeq 30$ for which $(\nu R^2)_f \approx 10^{-3}$ from Fig. 2.

Ott and Sudan suggest that helical ion orbits induced by traversing the converging field region may provide the reduction in axial energy-deposition length required to efficiently heat the plasma. Although this motion could be induced by decreasing L, radial excursions expected for the high values of $P_{\perp f}$ might be too large for useful heating of a 1 cm-radius plasma column. However, their suggestion of employing higher-atomic-number ions for range reduction would allow one to magnetically compress the beam in a way which maintains most of its energy in axial motion and limits radial excursions to values small compared to 1 cm.

VI. REFERENCES

1. P. Dreike, et al, "Proc. 6th International Conf. on Plasma Physics and Controlled Nuclear Fusion Research," Berchtesgaden, Federal Republic of Germany (International Atomic Energy Agency, 1976).
2. S. Humphries, T. J. Lee and R. N. Sudan, Appl. Phys. Lett. 25, 20 (1974); also J. Appl. Phys. 4, 187 (1975).
3. C. A. Kapetanakos, J. Golden, and W. M. Black, "Dependence of Ion Current on Voltage in a Reflex Triode," submitted to Phys. Rev. Lett.
4. S. J. Stephanakis, D. Mosher, G. Cooperstein, J. R. Boller, J. Golden, S. A. Goldstein, "Production of Intense Proton Beams in Pinched Electron Beam Diodes," submitted to Phys. Rev. Lett.
5. S. Humphries, R. N. Sudan, and L. Wiley, J. Appl. Phys. 47, 2382 (1976).
6. E. Ott and R. N. Sudan, Appl. Phys. Lett. 29, 5 (1976).
7. C. A. Kapetanakos, J. Golden and F. C. Young, Nuclear Fusion 16, 151 (1976).
8. M. J. Clauser, Phys. Rev. Lett. 35, 848 (1975).
9. G. Cooperstein, S. J. Stephanakis, J. R. Boller, R. Lee and S. A. Goldstein, Conf. Record-Abstracts of IEEE International Conf. on Plasma Sci., May 24-26, 1976, p. 123.
10. I. P. Shkarofsky, T. W. Johnston, and M. P. Bachynski, "The Particle Kinetic of Plasmas," (Addison-Wesley, Reading, Mass., 1966), Chap. 10.

11. J. M. Dawson, A. Hertzberg, R. E. Kidder, G. C. Vlases, H. G. Ahlstrom, and L. C. Steinhauer, "Proc. 4th Conf. on Plasma Physics and Controlled Nuclear Fusion Research," Madison, Wis. (International Atomic Energy Agency, Vienna, 1971), Vol. I, 673.

VII. APPENDIX

Here, the inclusion of electron pressure terms in the equations of motion are considered. The electron force-balance equation then takes the form[10]

$$Zen(\vec{E} + \vec{v} \times \vec{B}) + \vec{\nabla}\cdot\vec{\Pi} = 0 \tag{A1}$$

where

$$\vec{\Pi} = p_\perp \vec{I} + (p_{||}-p_\perp)\, \hat{e}_b \hat{e}_b \tag{A2}$$

and

$$\vec{v}\cdot\vec{\nabla}\left(\frac{p_\perp}{nB}\right) = \vec{v}\cdot\vec{\nabla}\left(\frac{p_{||}B^2}{n^3}\right) = 0 \tag{A3}$$

Here, $\hat{e}_b = \vec{B}/B$ is a unit vector in the magnetic-field direction. Since $(\vec{\nabla}\cdot\vec{\Pi})_\theta = 0$, Eq. (5), which states that the electron fluid follows the lines of force, still applies. Taking the scaler product of Eq. (A1) with $\vec{B}$ yields after some algebra and generous application of Maxwell's equations

$$Zen\left(B_r \frac{\partial}{\partial r} + B_z \frac{\partial}{\partial z}\right)\varphi - \left(B_r \frac{\partial}{\partial r} + B_z \frac{\partial}{\partial z}\right) p_{||}$$

$$+ \frac{p_{||}-p_\perp}{B}\left(B_r \frac{\partial}{\partial r} + B_z \frac{\partial}{\partial z}\right) B = 0. \tag{A4}$$

Employing Eq. (A3) allows this to be reduced to

$$\left(B_r \frac{\partial}{\partial r} + B_z \frac{\partial}{\partial z}\right)\left(\frac{p_\perp}{n} - Ze\varphi\right) + \frac{B}{n}\left(B_r \frac{\partial}{\partial r} + B_z \frac{\partial}{\partial z}\right)\frac{p_{||}}{B} = 0$$

since $\vec{B}\cdot\nabla\psi = 0$ follows from $\vec{v}\cdot\nabla\psi = 0$ and Eq. (5). Since $\frac{p_\perp}{nB}$ and $\frac{p_{||}B^2}{n^3}$

are constant along a line of force, and n is roughly proportional to B from Eq. (25), then $p_\perp \sim B^2$ ($\simeq B_z^2$ for the case at hand) while $p_{||} \sim B$ as the beam is compressed. If electrons in the injected beam are characterized by $p_{||} \approx p_\perp$ at $z = 0$, then $p_\perp$ will greatly exceed $p_{||}$ in the compressed beam. Also, since some tens of electron volts of temperature might be reasonable for the injected beam, $\frac{1}{2} m_e V_o^2 \gg kT_e$ at $z = 0$. Thus, if important at all, electron pressure effects will only be significant in the compressed beam where $p_\perp >> p_{||}$.

With the considerations of the last paragraph, it is reasonable to neglect $p_{||}$ in comparison with $p_\perp$ in Eq. (A5) so that

$$\left(B_r \frac{\partial}{\partial r} + B_z \frac{\partial}{\partial z}\right)\left(\frac{p_\perp}{n} - Ze\varphi\right) \simeq 0 \qquad \text{(A6)}$$

or

$$\frac{p_\perp}{n} - Ze\varphi \simeq S \frac{r^2}{2} B_z \qquad \text{(A7)}$$

in analogy with Eqs. (6), (7) and (14). But, from Eq. (A3), $\frac{p_\perp}{n} \sim B$ so that

$$Ze\varphi \simeq S \frac{r^2}{2} B_z + kT_{\perp o} \cdot \frac{B}{B_o} \qquad \text{(A8)}$$

where a constant temperature profile at $z = 0$ has been chosen.

It is seen that the maximum change in $Ze\varphi$ associated with initial electron temperature is of order $A \cdot kT_{\perp o}$ which is much too small to effect ion motion. The electron motion is only effected in azimuth through the temperature-dependence of the radial electric field which impacts only on the small self-field of the compressed beam. It is

therefore concluded that realistic electron temperatures do not effect the results of analysis in the body of this report.

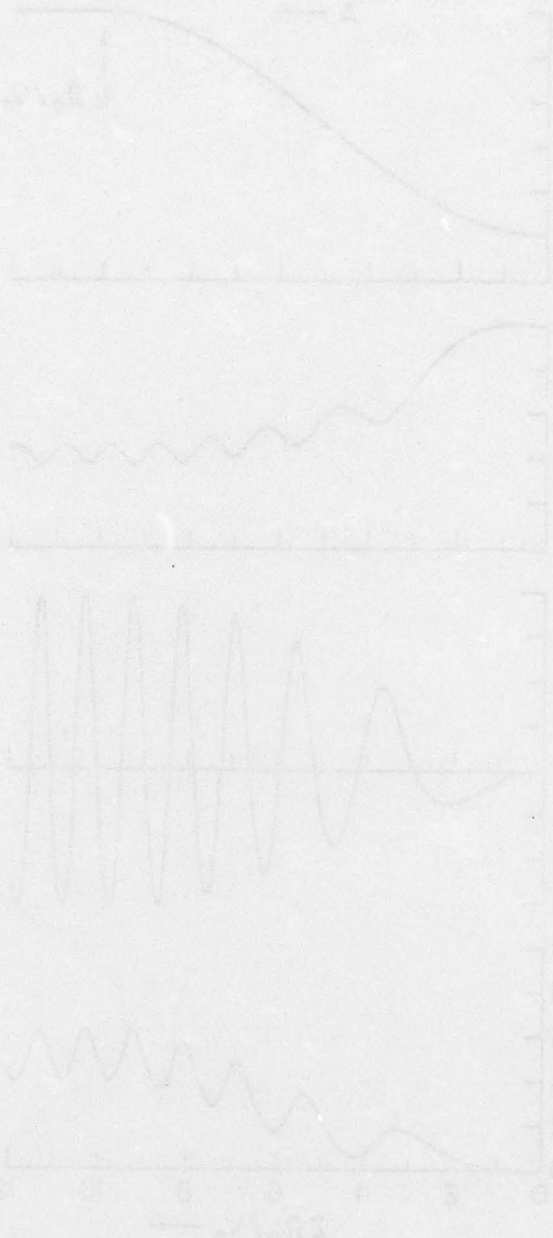

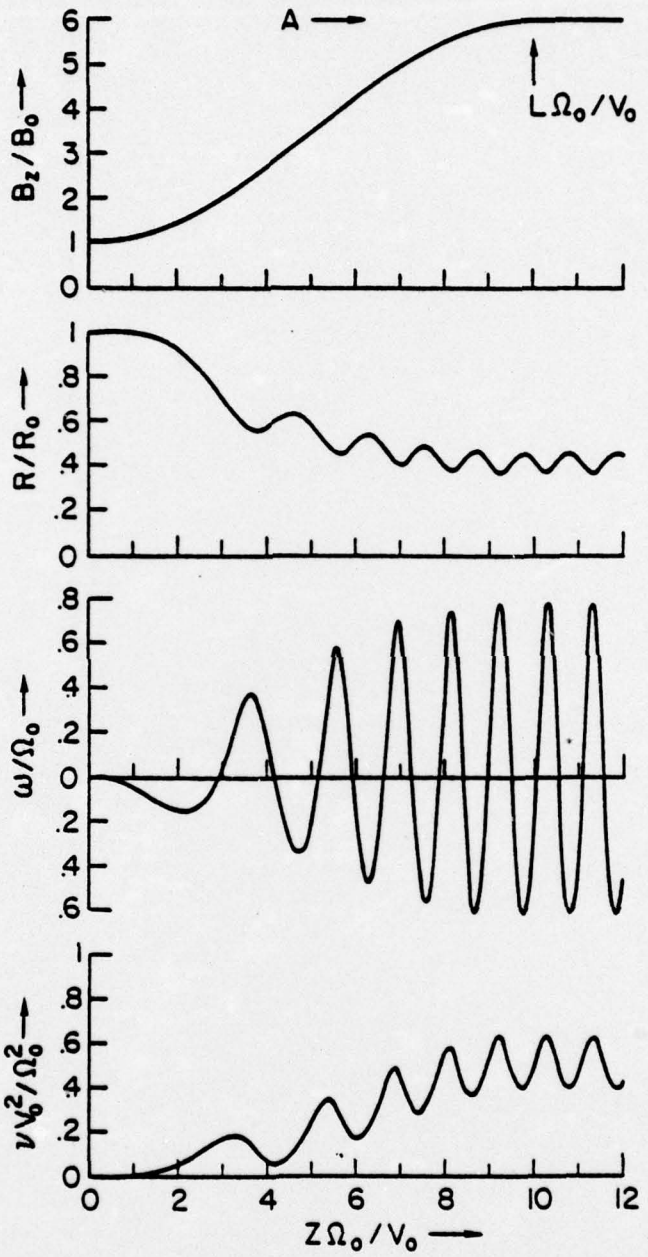

Fig. 1 — Variation of magnetic field strength B_z, beam envelope radius R, rotational frequency ω, and velocity-shear parameter ν with axial distance for a mirror ratio A = 6 and mirror length $L = 10\ V_0/\Omega_0$.

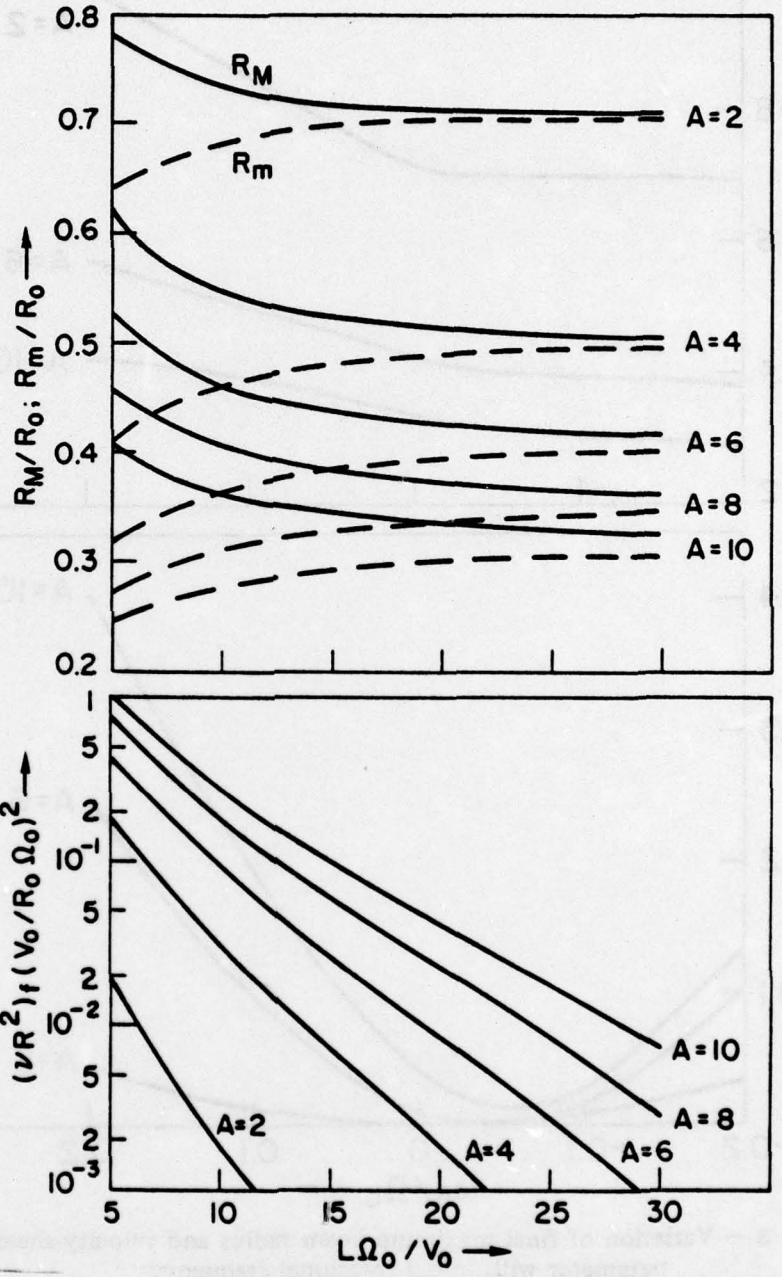

Fig. 2 — Variation of final beam-envelope extremum radii and velocity-shear parameter with mirror length for various values of the mirror ratio

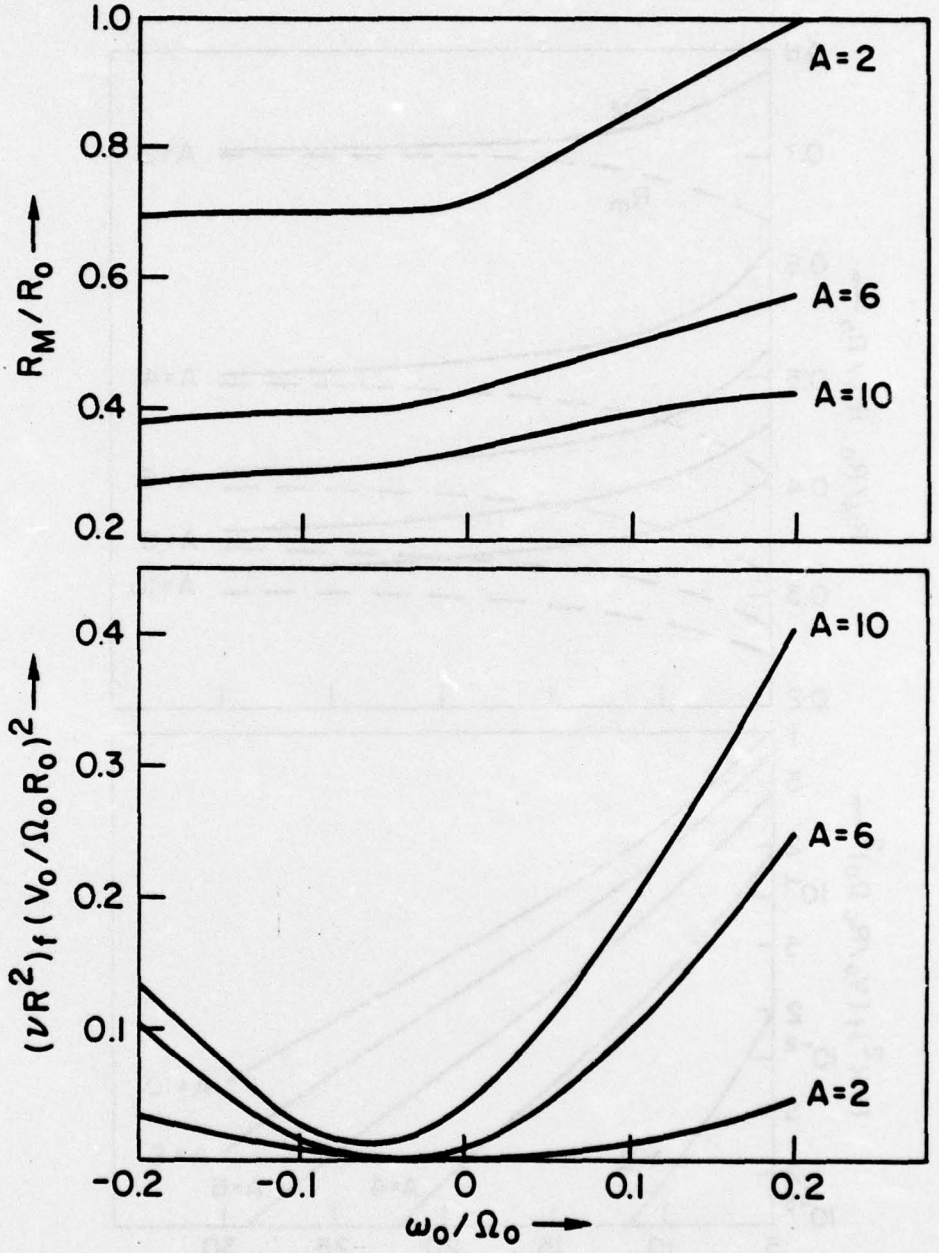

Fig. 3 — Variation of final maximum beam radius and velocity-shear parameter with initial rotational frequency

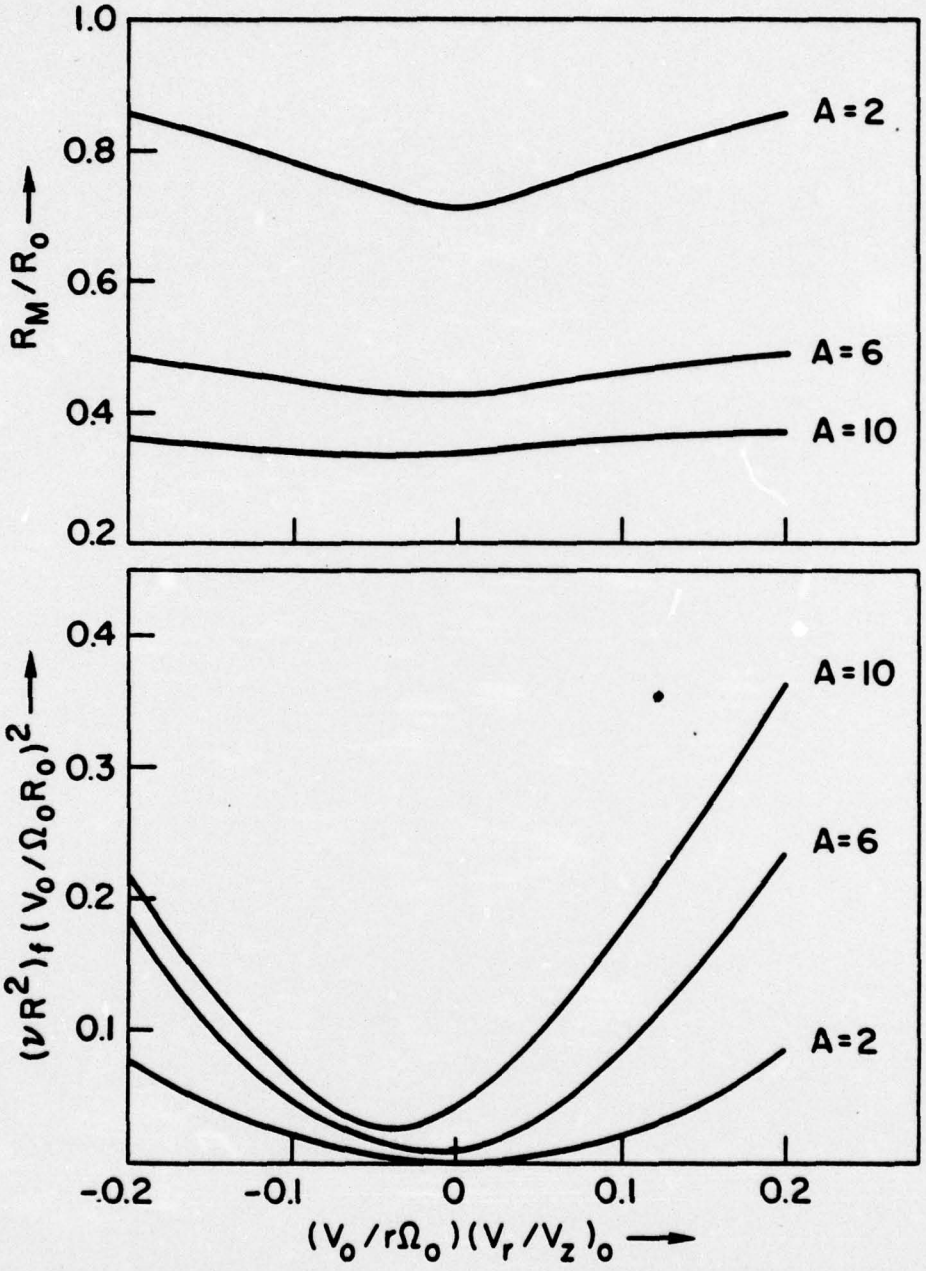

Fig. 4 — Variation of final maximum beam radius and velocity-shear parameter with initial beam convergence or divergence. Positive values of the abscissa indicate divergence.

DISTRIBUTION LIST

1. Director
Defense Advanced Research Projects Agency
Architect Building
1400 Wilson Boulevard
Arlington, Virginia 22209
Attn: LTC R. P. Sullivan

2. Director
Defense Nuclear Agency
Washington, D. C. 20305
Attn: DDST, Mr. Peter Haas
RATN
STTL, Technical Library (2 copies)
RAEV (2 copies)
STVL
STSI

3. Commander
Field Command
Defense Nuclear Agency
Albuquerque
Kirtland AFB, New Mexico 87115
Attn: FCPR

4. Chief
Field Command
Defense Nuclear Agency
Livermore Division
Box 808
Livermore, California 94550
Attn: FCPR-L

5. Director
Defense Research and Engineering
Washington, D. C. 20301
Attn: DAD (SK) Mr. G. R. Barse

6. Commander
Harry Diamond Laboratories
Adelphi, Maryland 20783
Attn: AMXDO-RBF, Mr. John Rosado
AMXDO-RBH, Mr. S. Graybill
AMXDO-RC, Dr. Robert Oswald, Chief, LAB 300

7. Air Force Weapons Laboratory, AFSC
Kirtland AFB, New Mexico 87117
Attn: DY, Dr. Guenther
EL, Mr. John Darrah
DYS, Dr. Baker
SAA
SUL, Technical Library
ELP, TREE Section

8. Space and Missile Systems Organization
Post Office Box 92960
Worldway Postal Center
Los Angeles, California 90009
Attn: SKT, Mr. Peter H. Stadler
RSP, System Defense and Assessment, LTC Gilbert

9. Sandia Laboratories
P. O. Box 5800
Albuquerque, New Mexico 87115
Attn: Document Control for 5220, Dr. J. V. Walker
Document Control for 5242, Dr. G. Yonas
Document Control for Technical Library

10. Aerospace Corporation
P. O. Box 92957
Los Angeles, California 90009
Attn: Mr. J. Benveniste
Dr. Gerald G. Comisar, Jr.

11. University of Texas
Fusion Research Center
Physics Building 330
Austin, Texas 78712
Attn: Dr. William E. Drummond

12. Battelle Memorial Institute
Columbus Laboratories
505 King Avenue
Columbus, Ohio 43201
Attn: Mr. P. Malozzi

13. Maxwell Laboratories, Inc.
9244 Balboa Avenue
San Diego, California 92123
Attn: Dr. P. Korn

14. Mission Research Corporation
735 State Street
Santa Barbara, California 93101
Attn: Dr. Conrad L. Longmire

15. Physics International Corporation
2700 Merced Street
San Leandro, California 94577
Attn: Document Control for Dr. Sidney Putnam
Document Control for Mr. Ian Smith

16. R & D Associates
P. O. Box 9695
Marina del Rey, California 90291
Attn: Dr. Bruce Hartenbaum

17. Science Applications, Inc.
P. O. Box 2351
La Jolla, California 92037
Attn: Dr. J. Robert Beyster

18. Stanford Research Institute
333 Ravenswood Avenue
Menlo Park, California 94025
Attn: Dr. Robert A. Armistead, Jr.

19. Dr. Victor A. J. Van Lint
Mission Research Corporation
7650 Convoy Court
San Diego, California 92111

20. Commander
Naval Surface Weapons Center
White Oak Laboratory
Silver Spring, Maryland 20910

21. DASIAC, GE Tempo
El Paseo Building
816 State Street
Santa Barbara, California 93102

22. DDC (2 copies)

23. Code 2628 (20 copies)

24. Code 7700

25. Code 7770 (20 copies)